The fate of polar trace organic compounds in the hyporheic zone

Jonas L. Schaper, Wiebke Seher, Gunnar Nützmann, Anke Putschew, Martin Jekel, Jörg Lewandowski

https://orcid.org/0000-0001-5278-129X

Citation

Schaper JL, Seher W, Nützmann G, Putschew A, Jekel M, Lewandowski J. The fate of polar trace organic compounds in the hyporheic zone. Water Research. 2018;140:158-66.

The fate of polar trace organic compounds in the hyporheic zone

Jonas L. Schaper[1,2]*, Wiebke Seher[1], Gunnar Nützmann[1,3], Anke Putschew[2], Martin Jekel[2] and Jörg Lewandowski[1,3]

[1] Leibniz-Institute of Freshwater Ecology and Inland Fisheries, Department Ecohydrology, Müggelseedamm 310, 12587 Berlin, Germany

[2] Technical University of Berlin, Chair of Water Quality Engineering, Strasse des 17. Juni 135, 10623 Berlin, Germany

[3] Humboldt University Berlin, Geography Department, Rudower Chaussee 16, 12489 Berlin, Germany

*corresponding author; schaper@igb-berlin.de, Leibniz-Institute of Freshwater Ecology and Inland Fisheries, Department Ecohydrology, Müggelseedamm 310, 12587 Berlin, Germany

Abstract

The hyporheic zone (HZ) is often considered to efficiently remove polar trace organic compounds (TrOCs) from lotic systems, mitigating potential adverse effects of TrOCs on ecosystem functioning and drinking water production. Predicting the fate of TrOCs in the hyporheic zone (HZ) is difficult as the in-situ removal rate constants are not known and the biogeochemical factors as well as hydrological conditions controlling the removal efficiency are not fully understood. To determine the in-situ removal efficiency of the HZ for a variety of TrOCs as a function of the biogeochemical milieu, we conducted a field study in an urban river near Berlin, Germany. Subsurface flow was studied by time series of temperature depth profiles and the biogeochemical milieu of the HZ by concentration depth profiles. These results, in conjunction with a 1D advection-dispersion transport model, were used to calculate first-order removal rate constants of several polar TrOCs in the HZ. For the majority of TrOCs investigated, removal rate constants were strongly dependent on redox conditions, with significantly higher removal rates observed under predominantly suboxic (i.e. denitrifying) compared to anoxic (i.e. Fe and Mn reducing) conditions. Compared to previous studies on the fate of TrOCs in saturated sediments, half-lives within oxic/suboxic sections of the HZ were relatively low, attributable to the site-specific characteristics of the HZ in a stream dominated by wastewater treatment plant effluent. For nine out of thirteen investigated TrOCs, concentrations decreased significantly in the HZ with relative removal percentages ranging from 32% for primidone to 77% for gabapentin. For many TrOCs, removal efficiency decreased drastically as redox conditions became anoxic. For the majority of compounds investigated here, the HZ indeed acts as an efficient bioreactor that is capable of removing TrOCs along relatively short flow paths. Depending on the TrOC, removal capacity may be enhanced by either increasing the magnitude of groundwater-surface exchange fluxes, by increasing the total residence time in the HZ or the exposure time to suboxic zones, respectively.

35 **Keywords**

36 Pharmaceuticals, organic micropollutants, biotransformation, urban water cycle, removal efficiency

Introduction

Trace organic compounds (TrOCs) derived from wastewater treatment plants (WWTP) are frequently detected in surface waters in which they impair ecosystem functioning (Schwarzenbach et al., 2006) and pose risks for drinking water production, especially in urban areas where water cycles might be partially closed (Pal et al., 2014). The hyporheic zone (HZ), the interface between groundwater and surface water in streams, has often been considered to efficiently remove TrOCs (Lewandowski et al., 2011). Depending on the magnitude and direction of groundwater-surface water exchange and hyporheic exchange fluxes, the HZ may contribute to the overall attenuation of TrOCs in streams (Riml et al., 2013; Writer et al., 2013) and may act as a reactive barrier protecting groundwater from surface water pollution and vice versa (Huntscha et al., 2013).

Quantitative information on the reactivity of TrOCs in saturated sediments, often expressed as first-order removal rate constants, predominantly originates from either laboratory experiments (Burke et al., 2014; Li et al., 2015; Radke and Maier, 2014) or bank filtration studies (Henzler et al., 2014; Huntscha et al., 2013). For many TrOCs, reported removal rate constants were found to be highly site- and experiment specific and varied up to three orders of magnitude among different subsurface environments and experimental setups (Greskowiak et al., 2017). It has further been shown that a variety of physical and biogeochemical factors, such as temperature (Burke et al., 2014), redox conditions (Wiese et al., 2011), concentrations of labile dissolved organic carbon (DOC) (Hoppe-Jones et al., 2012) and the abundance and diversity of microorganisms (Bertelkamp et al., 2016) may influence the reactivity of TrOCs in saturated sediments.

Compared to other subsurface environments, hyporheic zones are typically characterized by intense microbial activity, diverse microbial communities and steep redox gradients (Boano et al., 2014). Field investigations that link the fate of TrOCs to the distinct biogeochemical characteristics in the HZ, are widely lacking and thus, in-situ removal rate constants of TrOCs in the HZ are not known. Removal efficiency of the HZ is generally not only a function of the removal rate constants and thus the

62   biogeochemical milieu, but also of the time over which an attenuation reaction can take place (i.e. the

63   residence time). The spatial distribution of biogeochemical parameters, such as the ambient redox

64   potential in the HZ, is often tightly coupled to flow characteristics. Compared to bank filtration systems,

65   residence times in the HZ are usually much shorter. The in-situ interactions between transport timescales

66   in the HZ and the biogeochemical conditions that control the ambient reactivity of TrOCs in HZ, (i.e. the

67   factors that govern the efficiency of the HZ in removing polar TrOCs) are poorly understood.

68   The present study had two aims: (i) providing in-situ first-order removal rate constants for several TrOCs

69   for the HZ of an urban lowland stream and (ii) determine the hydrological and biogeochemical factors that

70   limit the efficiency of the HZ in removing TrOCs. To this end, in-situ first-order removal rate constants

71   are determined for a variety of polar WWTP derived TrOCs under different redox conditions.

72   We hypothesize that in a river that is dominated by WWTP effluent removal rate constants in the

73   hyporheic zone substantially deviate from rates obtained in laboratory studies and bank filtration systems.

74   As reaction rates for many compounds are likely to be redox-dependent, reaction rates are expected to be

75   strongly controlled by redox conditions in the HZ. Consequently, removal efficiency is likely to depend on

76   both the extent of redox zones as well as on the magnitude of groundwater-surface exchange and

77   hyporheic exchange fluxes.

78 **Methods**

79 **2.1 Site description**

80 River Erpe is an urban lowland river, located at the eastern edge of Berlin, Germany, that receives

81 between 60% and 80% of its discharge from the large municipal WWTP Münchehofe. A detailed

82 description of river morphology and general biogeochemical traits of River Erpe can be found elsewhere

83 (Lewandowski et al., 2011). The study site is located at Heidemühle (Lat: 52.478647, Long: 13.635146)

84 roughly 1 km downstream of the confluence of River Erpe and the WWTP Münchehofe effluent.

85 Streambed morphology at the field site was dominated by small dunes (crest height < 5 cm) and

86 macrophyte cover during the study period was $< 10\%$. Streambed sediment characteristics were

87 determined from one 30 cm long core per station taken in close proximity (< 10 cm) to the sampling

88 station using a hand auger (9.0 cm ID). Saturated hydraulic conductivities (K) at 10 °C, measured using a

89 KSAT device (UMS Munich), were found to be log-normally distributed with a mean value of 5.0×10^{-5}

90 m s^{-1} and a standard deviation of 7.4×10^{-5} m s^{-1}. Mean sediment porosity calculated from oven dried

91 samples was 0.39 ± 0.1. Organic carbon content (f_{oc}), determined by loss on ignition, ranged between 0.5

92 and 6 wt.% and was found to be log-normally distributed with a mean value of 2.4 ± 2.7 wt.%.

93 **2.2 Experimental setup overview and field investigation periods**

94 The experimental setup consisted of six stations (S1 – S6) located close to the south-eastern bank of River

95 Erpe (Figure 1a). Each sampling station was equipped with a ring enclosure (PVC pipes with a diameter

96 of 15 cm and a height of 32 cm) which was inserted vertically into the sediment, with the top rim of the

97 pipe being level with the sediment surface. Concentrations of TrOCs in effluent-receiving streams are

98 typically variable in time as both concentrations of TrOCs in WWTP effluent itself as well as the relative

99 proportion of WWTP effluent to overall stream discharge may change on a sub-daily and daily basis

100 (Lewandowski et al., 2011). To overcome this challenge, we used dialysis chambers, also called peepers

101 (Hesslein, 1976), a passive sampling technique that integrates porewater solute concentrations over a time

span of several days and thus allows the sampling of time integrated, quasi-steady-state concentration depth profiles in the hyporheic zone. A detailed description on the functionality of peepers and their applicability to sample TrOCs in the hyporheic zone is provided in the Supplementary Material (SM). Between December 1st and December 15th, 2015, peepers were used to collect porewater depth profiles in the hyporheic zone (details below, section 2.4). To sample porewater both within the ring enclosure and outside of the ring enclosure, one peeper was inserted into the sediment within the ring enclosure and one inserted directly adjacent to the first one but outside of the ring enclosure (Figure 1 b). Between December 1st 2015 and April 15th, 2016, temperature probes (details below, section 2.3) were installed inside and outside the ring enclosures. Vertical seepage flux inside the ring enclosure at S1, S2, S3, S4 and S6 as well as outside ring enclosures at S3 was calculated from field temperature data measured between December 1st 2015 and December 15th 2015. Due to a limited availability of temperature probes, vertical seepage fluxes inside ring enclosure at S5 and outside ring enclosures at S1, S2, S4, S5 and S6 were calculated from temperature data collected between January 5th and April 15th 2016. This approach was justified as (i) head gradients between river stage and the riparian aquifer were close to time invariant on timescales of weeks and months and (ii) flux measurements made at the same station and peeper position between December 2015 and April 2016 showed only little variation. A detailed summary of deployment periods and the respective hydrodynamic conditions of the River Erpe between December 2015 and April 2016 can be found in the SM. The original purpose of the ring enclosures was to limit the influence of potential horizontal subsurface flow in the hyporheic zone. However, flow investigations (sections 2.3.2 and 3.1) did not indicate the presence of strong horizontal flow components outside the ring enclosures. As a result, the same reactive transport model was used to evaluate concentration profiles both inside and outside the ring enclosures. Stream stage, temperature and electrical conductivity (EC) were measured continuously every 5 min between December 1st, 2015 and April 15th, 2016 using a CTD Diver (Van Essen Instruments B.V., Netherlands) installed in a stilling well (SW1, Figure 1a). Between February 8th and April 15th, additional head measurements were performed using a Pressure Diver (Van Essen Instruments B.V.,

127   Netherlands) in a second stilling well (SW2, Figure 1a) and a groundwater observation well (GW, Figure

128   1a). Head measurements were performed to gain general information on groundwater-surface water

129   interactions at the field site and qualitatively confirm the temperature based flux calculations (section 2.3).

130   Stream stage at SW2 during peeper deployment was inferred from correlations of stream stages at SW1

131   and SW2 between February 8th and April 15th 2016 (Figure SM-02).

132   Daily variations of stream stage and EC showed a periodic saw-toothed pattern with stage and EC troughs

133   in the early morning and peaks around noon and in the afternoon (Figure SM-08). Water levels in the river

134   were consistently above groundwater level, even during early morning stage troughs. As a consequence,

135   the groundwater-surface water interactions were characterized by downwelling conditions, a finding

136   which is in qualitative agreement with the flux calculations in section 2.3.

137

138
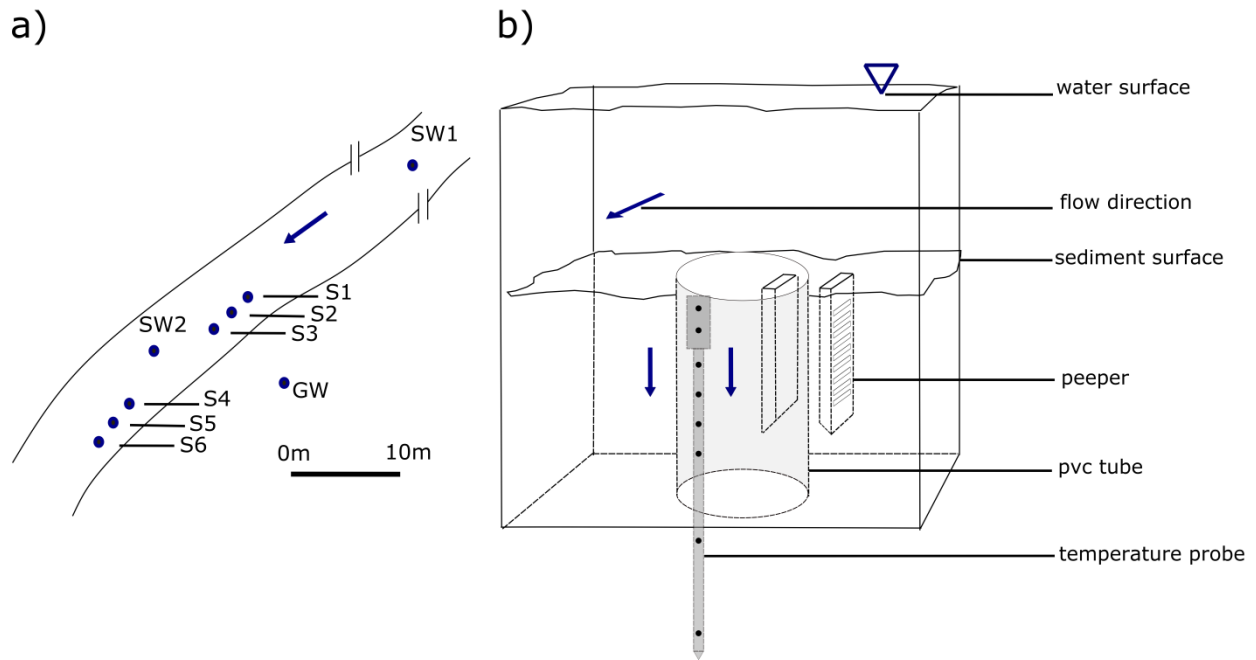
Figure 1 a) Study site with stations (S1 – S6) close to south-eastern bank of River Erpe. Surface water stilling well 1 (SW1) is approximately 100 m upstream of S1 while surface water stilling well 2 (SW2) is located between S3 and S4. A groundwater well (GW) with filter screen 1.5 m below the water table is located 5 m beside the river. b) Each of the six stations S1 – S6 consists of a 32 cm long PVC pipe (ring enclosure) with its upper end being level with the sediment – water interface. Porewater samplers, so-called peepers, are placed next to each other inside and outside of the pipe, with the closed side of each peeper facing towards the PVC wall. Blue arrows indicate predominant flow directions.

2.3 Calculation of vertical seepage fluxes and transport parameters

2.3.1 Measurements of temperature time series

Temperature depth profiles were obtained using Multi Level Temperature Sticks (MLTS, UIT, Dresden), which are described in detail by Munz et al., (2011). In brief, MLTS sticks are polyoxymethylene sticks of a total length of 0.66 m and a diameter of 0.02 m, which are equipped with eight TSIC-506 temperature sensors (accuracy 0.07 °C between 5 °C and 45 °C). The probes were placed vertically in the streambed, with the head of the temperature stick being level with the sediment surface. Temperature time series where obtained for sediment depths 7, 17, 22, 27, 32, 42 and 62 cm.

153   2.3.2 Calculation of vertical seepage fluxes using VFLUX 2.0

154   Vertical seepage flux estimates based on continuous time series of temperature depth profiles were

155   evaluated using the MATLAB code VFLUX 2.0 (Gordon et al., 2012). In brief, VFLUX 2.0 utilizes

156   dynamic harmonic regression (DHR) (Young et al., 1999) to extract amplitude damping ratios (A_r) and

157   phase shifts ($\Delta\varphi$) from two sinusoidal temperature time series measured at two different depths within the

158   stream sediment. DHR is a general case of the harmonic regression model in which the trigonometric

159   parameters describing the frequency components of the raw temperature time series may vary over time.

160   In the present study we used the combined $A_r\Delta\varphi$ method introduced by McCallum et al., (2012) to

161   calculate seepage fluxes.

162   Vertical seepage flux was evaluated at 2 h intervals between sensors in 7 and 17, 17 and 27 cm depth

163   resulting in center-of-pair depths of 12 and 22 cm, thus covering the depth range of porewater sampling.

164   Monte Carlo Analysis was performed using the "vfluxmc" function implemented in VFLUX 2.0. Mean

165   seepage flux rates were calculated by first averaging flux over depth and then averaging depth-integrated

166   fluxes over time. To minimize errors induced by DHR filtering, the first and last 24 h of flux results were

167   discarded. Since VFLUX provides Darcy fluxes (q), calculated flux rates were divided by the average

168   porosity to derive porewater velocities (v).

169   2.3.3 Calculation of dispersion coefficients

170   Based on the calculated porewater velocities, the respective effective hydrodynamic dispersion

171   coefficients (D) were calculated via:

$$D = \tau D_{mol} + \alpha_L v \tag{1}$$

172

173

174   in which τ denotes the tortuosity, D_{mol} the molecular diffusion coefficient, v the porewater velocity and α_L

175   the longitudinal dispersivity. Tortuosity τ was assumed to be 0.7 and α_L was set to a tenth of the profile

176   length (2 cm). As D_{mol} for the respective TrOCs are generally smaller than 10^{-9} m^2 s^{-1} (Table SM-09) and

10

177   porewater velocities measured in the present study were larger than 10^{-6} m s^{-1} (Table 1), the contribution

178   of D_{mol} to overall hydrodynamic dispersion coefficients was found to be negligible and thus molecular

179   diffusion was omitted in further calculations.

180   **2.4 Water sampling and analysis**

181   Deployed peepers (2.5 cm x 9.5 cm x 26.5 h x w x l) contained 20 chambers (approx. 10 mL of chamber

182   volume) in 1 cm increments. The chambers were filled with deionized water and covered with a

183   permeable membrane (polysulfon, 0.2 μm HT Tuffryn 200, Pall Corporation). Prior to installation, peepers

184   were placed into oxygen free water to reduce oxygen input into streambed sediments. In contrast to

185   common sampling practice the peepers had to be inserted completely into the sediment, because first trials

186   revealed a scouring around peepers if they were reaching into the overlying water. Thus, the peepers did

187   not sample overlying water or the immediate sediment-water interface. Peeper chambers were sampled on

188   site chamber by chamber immediately after recovery from the sediment using a needle and a 10 ml

189   syringe. Two ml of sampled porewater from each chamber were used for TrOC analysis, 2 ml were used

190   for nitrate analysis and 3 ml were used for major cation analysis. At SW1 an automatic water sampler

191   (model 3700, Teflon suction line, Teledyne ISCO, Lincoln, NE.) was deployed to take surface water

192   samples from December 1st to December 15th. Approximately 350 ml of surface water were collected

193   every hour from 20 cm below the water surface. Samples were combined in a flow proportional manner

194   based on stream stage derived hourly discharge, yielding a flow-weighted surface water sample for each

195   day during the peeper deployment period. Details on discharge measurements and the rating curve can be

196   found in the SM. Integrated water samples were used to measure time series of surface water pH, TrOCs

197   and major cation concentrations. Details on sample filtering and storage are provided in the SM.

198   The TrOCs studied include the pharmaceuticals gabapentin (GAB), bezafibrate (BZF), diclofenac (DCF),

199   venlafaxine (VLX), 4-formylaminoantipyrin (FAA), primidone (PRI), carbamazepine (CBZ), and

200   metoprolol (MTP) as well as the artificial sweetener acesulfame (ACS) and two benzotriazoles (1H-

201   Benzotriazole, BTA, and 5-Methylbenzotriazole, MBT), which are mostly used as anti-corrosion agents.

11

202 TrOCs were measured via high performance liquid chromatography with tandem mass spectrometry

203 (HPLC-MS/MS) following a method established previously (Zietzschmann et al., 2016, 2015). Separation

204 was achieved on a XSelect HSS T3 HPLC column (2.5 μm particle size, 2.1 * 50 mm, Waters, USA)

205 using a linear gradient (ultra pure water with 5 vol.-% methanol (HPLC grade, J.T. Baker, USA) and 0.1

206 vol.-% formic acid (HPLC grade, Sigma Aldrich, Germany) versus 100% methanol). A TSQ Vantage

207 mass spectrometer (Thermo Fisher Scientific, USA) in ESI ± modes was used for compound analysis.

208 Each TrOC was identified by the characteristic ratio of the peak areas of two fragments, which were

209 chosen according to the DAIOS database (Zweckverband Landeswasserversorgung, Stuttgart, Germany).

210 For TrOC quantification, deuterated internal standards (Toronto Research Chemicals, Canada) were used

211 in combination with the more abundant fragment ion. Calibration curves consisted of 9 standards that

212 ranged from 0.01 to 55 µg/L and were fitted using a weighted (1/x) linear regression model (coefficients

213 of determination, R^2, were always > 0.99). Limits of quantification (LOQs, Table SM-01) were set to the

214 calibration level at which the less abundant fragment ion showed a signal to noise ratio of $\geq$ 3. Data

215 evaluation was performed with Xcalibur 2.1 (Thermo Scientific). Additional details on the method are

216 provided in the SM.

217 Major cations and dissolved iron concentrations were determined via inductively coupled plasma optical

218 emission spectrometry (ICP-OES, ICP iCAP 6000series, Thermo Fisher). Nitrate-N was measured using a

219 continuous-flow-analyser (SAN ++, Skalar) after DIN EN ISO 13395. For each surface water sample, pH

220 was determined using a handheld pH meter, calibrated prior to each use (SenTix 41, WTW).

221 **2.5 Modeling of removal rate constants**

222 The one-dimensional advection-dispersion transport equation including first-order decay was used to

223 calculate removal rate constants of TrOCs from porewater depth profiles. Assuming steady-state

224 conditions in a homogeneous medium, negligible retardation of TrOCs along flow paths and uniform flow

225 conditions, the 1D advective-dispersion transport equation can be written as:

226

$$0 = D\frac{d^2c}{dx^2} - v\frac{dc}{dx} - kc \tag{2}$$

227

228 In which v denotes the vertical porewater velocity (m s^{-1}), D the effective hydrodynamic dispersion

229 coefficient (m^2 s^{-1}) and k the first-order removal rate constant (s^{-1}). Assuming that the solute concentration

230 is zero at infinite depth, the solution to Equation 4 can be written as:

231

$$c(x) = c_{in}e^{\frac{v-\sqrt{v^2+4Dk}}{2D}x} \tag{3}$$

232

233 In which c_{in} denotes an arbitrary input concertation at the sediment-water interface. Following

234 linearization, the exponent of Equation 3 was found by fitting a linear model to the concentration data

235 using the statistical software package R (R Core Team, 2016). Details on the derivation of the analytical

236 solution (Equation 3) and parameterization can be found in the SM. It should be noted that the removal

237 rate constant (k), although mathematically treated as a first-order constant, actually represents a pseudo

238 constant, as it integrates a variety of attenuation processes. Removal rate constants were set to zero if the

239 relative removal within one profile or sub-profile was smaller than two times the associated standard

240 deviation. For calculation purposes, if the concentration of a compound in a depth profile was below the

241 LOQ, its concentration was set to the respective LOQ. Model assumptions are considered to be reasonably

242 well met as hydrological conditions and concentrations of TrOCs in the surface water remained relatively

243   constant over the peeper sampling period (Figures SM-08 & 11). Under these conditions peepers are likely

244   to sample quasi-steady-state concentration profiles in the HZ. As the majority of TrOCs investigated in the

245   present study are either neutral or negatively charged under ambient pH (pH = 7.7), electrostatic

246   interactions between TrOCs and hyporheic material are considered to be negligible. The investigated

247   TrOCs were further characterized by low $logD_{ow}$ values (Table SM-10) and thus retardation of TrOCs in

248   the HZ due to partitioning into sediment organic matter is likely to be small. Even for compounds that

249   show comparatively high $logD_{ow}$ values, such as CBZ and BTA, previous field studies found very low

250   retardation factors (Huntscha et al., 2013). Concentration time series of TrOCs in the surface water as well

251   as a detailed discussion of the relevance of sorption and the assumption of quasi-steady state are provided

252   in the SM. Since the study site was characterized by consistent downwelling (sections 2.2 and 3.1),

253   concentration data were not corrected for dilution with riparian groundwater. In order to compare removal

254   rate constants to literature values, compound half-lives were calculated according to:

$$t_{1/2} = \frac{\ln(2)}{k} \tag{4}$$

255

3. Results and Discussion

3.1 Transport characteristics in the hyporheic zone

The mean vertical porewater velocity (positive = downward) ranged from 0.12 m d^{-1} inside S4 to 0.89 m d^{-1} inside S2 (Table 1). Fluxes at S2, S3, S4, S5 and S6 showed no difference with peeper position (i.e. inside and outside ring enclosures), while the flux calculated outside S1 was only half the flux calculated inside S1.

Table 1 Mean values ± standard deviations of porewater velocities (v) for the different sampling stations and inside/outside ring enclosures. Porewater velocities were calculated by dividing VFLUX derived Darcy velocities by sediment porosity.

Station	v	
	m d^{-1}	
	inside	outside
S1	0.84 ± 0.32	0.36 ± 0.13
S2	0.89 ± 0.31	0.83 ± 0.34
S3	0.84 ± 0.29	0.85 ± 0.30
S4	0.12 ± 0.05	0.25 ± 0.08
S5	0.59 ± 0.22	0.65 ± 0.24
S6	0.78 ± 0.29	0.81 ± 0.30

265   The mean vertical seepage fluxes measured inside and outside the ring enclosures were well within the

266   range reported in similar studies (Fitzgerald et al., 2015; Gordon et al., 2012) and matched downward

267   seepage rates previously calculated for the same river stretch (Lewandowski et al., 2011). During the

268   entire investigation period (December 2015 – April 2016) flux estimates indicated positive (downward)

269   flux which is consistent with the general head gradient at the study site, indicating downward flux from

270   the river to the riparian aquifer (section 2.2).

271   Errors associated with the calculation of vertical seepage fluxes using the McCallum $A_r \Delta \varphi$ method mainly

272   result from non-ideal field conditions that violate model assumptions, such as non-uniform, non-steady

273   and multidimensional flow. As the ring enclosure only allows purely vertical and uniform flow, the model

274   assumptions of uniform one-dimensional flow fields are highly likely to be met for fluxes measured inside

275   ring enclosures. However, the flow field outside the ring enclosures could have been subjected to both

276   vertical and horizontal flow components. Additional model calculations indicated that horizontal

277   hyporheic exchange induced by small sand dunes and ripples was < 0.05 m d^{-1} (see SM for details).

278   Moreover, fluxes calculated inside ring enclosures resembled fluxes outside ring enclosures for all stations

279   but S1. It is thus unlikely that horizontal flow components significantly distorted the flow field outside

280   ring enclosures. Additional errors induced by non-steady flow conditions as well as non-ideal sensor

281   spacing and sensor accuracy were found to be of minor importance (see SM for detailed discussion).

282   We conclude that the vertical seepage fluxes calculated by the McCallum $A_r \Delta \varphi$ method are likely to

283   resemble the actual vertical seepage fluxes quite well. Consequently, differences between sites and peeper

284   positions result likely from sediment heterogeneity and the associated variability in hydraulic

285   conductivity.

3.2 Redox zonation in the HZ

Nitrate concentrations were high in the surface water (median NO_3^--N concentration 3.5 mg/L, Table SM-07) and decreased rapidly within the streambed sediments. The only exception is the profile outside S2, in which nitrate concentrations remained relatively constant. As nitrate was depleted, concentrations of total dissolved iron and dissolved manganese (Fe_{tot}, Mn) increased (Figure SM-12). The depth ranges between the sediment-water boundary and the depth at which nitrate was completely depleted as well as the range between the depth at which Mn and Fe_{tot} concentrations increased and the lower end of the peeper were considered to mark the extent of oxic to suboxic and anoxic redox conditions within the HZ (Figure SM-12, Figure 2). The mean extent of oxic/suboxic and anoxic sub-sections in the HZ was 11 ± 4 cm and 10 ± 3 cm, respectively. The rapid consumption of surface water borne electron acceptors along relatively short flow paths and hence the development of steep redox gradients at the surface water-streambed interface is typical for hyporheic zones (Krause et al., 2017) and in agreement with previous studies on sediment biogeochemistry conducted at River Erpe (Lewandowski et al., 2011).

The spatial extent of the redox zonation, i.e. the depth and steepness of the redoxcline, is generally a function of both transport characteristics as well as biogeochemical parameters, such as the quality and abundance of electron donors and acceptors, microbial turnover rates or the content of sediment organic matter. In previous field investigations higher exchange fluxes led to deeper oxygen penetration depths and later onset of denitrification (Harvey et al., 2013). The relatively steep redox gradients inside the ring at S4 and S5 correspond qualitatively to lower seepage fluxes measured inside the ring enclosures at these stations. However, redox profiles inside the ring enclosures at S1 and S2 as well as redox profiles inside and outside S2, S5 and S6 were remarkably different, although vertical seepage rates were similar. Overall, no quantitative correlation was found between calculated vertical seepage flux rates and the extent of redox zones as shown in Figure 2. Since high resolution measurements of sedimentological characteristics of Erpe sediment were not available, it is difficult to differentiate between the combined effects of sedimentary and hydrological controls on redox zonation. The spatial variability of sediment

311 organic matter (f_{oc}) in the HZ of River Erpe, however, was relatively high (Figure SM-14). It therefore

312 seems likely that the spatial extent of redox zonation is not only a function of the magnitude of vertical

313 seepage flux but is also to a large extent controlled by the spatial distribution of sediment organic matter.

3.3 Reactivity of TrOCs in the HZ

Removal rate constants were calculated over the entire profile range and for each redox zone (suboxic and anoxic) shown in Figure 2. Note that the profile taken outside S2 was excluded as oxic conditions prevailed and no denitrification was observed. Kruskal-Wallis tests demonstrated that for all compounds but SMX, DTA, CBZ and VLX removal rate constants derived for suboxic conditions were significantly larger (p < .05) than the ones calculated for anoxic conditions (Table 2). Consequently, for TrOCs that showed redox-dependent attenuation, removal rate constants are only reported for the respective redox conditions. Median half-lives obtained from oxic/suboxic conditions varied between 0.43 d for PRI and 0.04 d for GAB (Table 2). General stability of TrOCs in the suboxic zone was in the order GAB < ACS ≈ BZF < BTA < DCF < MBT < PRI. Median half-lives for the same set of compounds calculated from anoxic sections of the profile did not differ from zero or were even negative. Depth profiles of gabapentin, associated model fits as well as the spatial extent of oxic/suboxic and anoxic zones are shown in Figure 2. Depth profiles for the remaining TrOCs, individual removal rate constants calculated from every (sub-) profile and a comparison of TrOC concentrations measured in the present study to concentrations previously measured in River Erpe are provided in the SM. Due to analytical difficulties, removal rate constants and respective half-lives for ACS and VLX were only calculated from eight profiles.
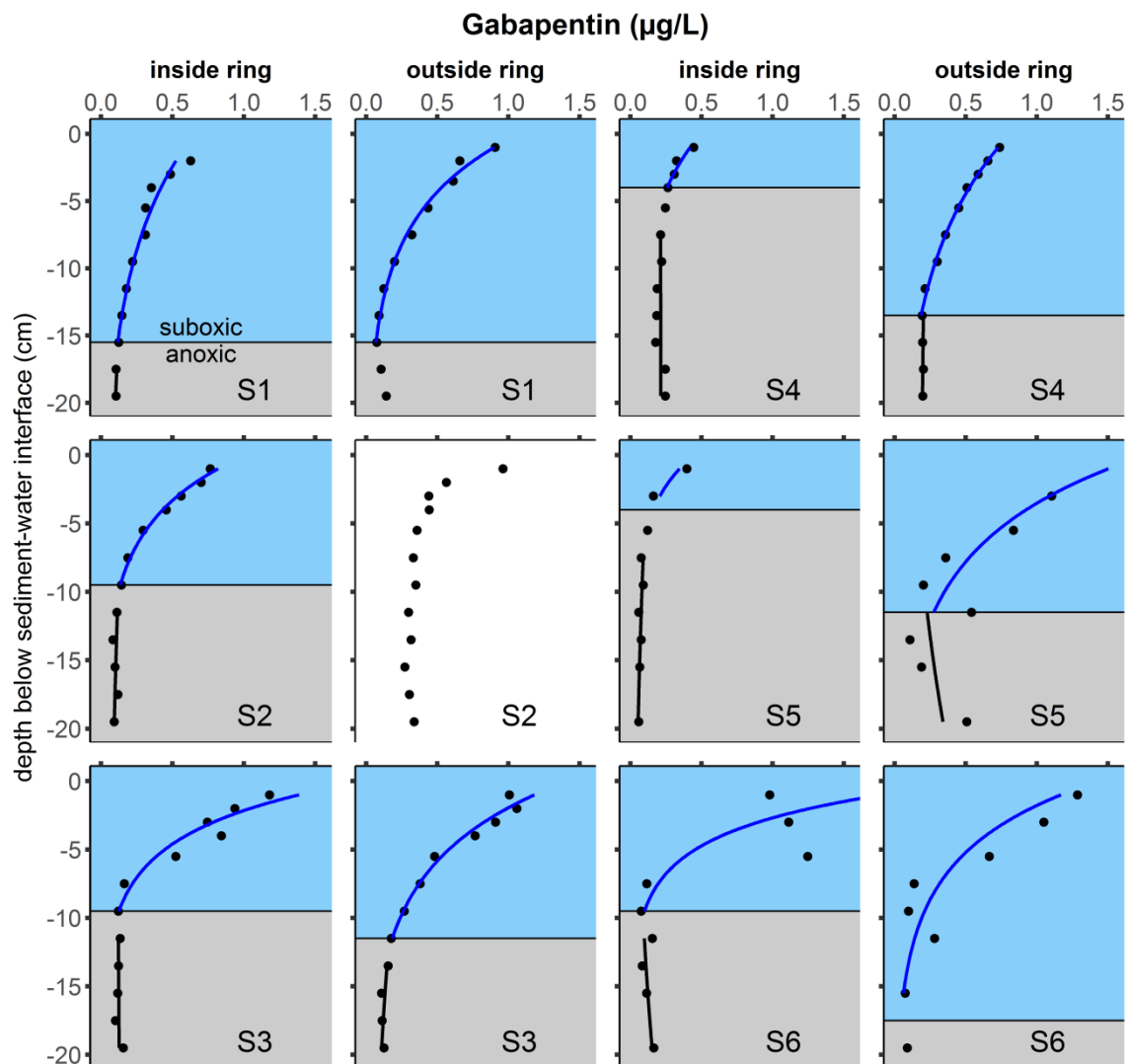
Figure 2 Equilibrium depth profiles of gabapentin (black dots) at the different sampling stations and inside/outside ring enclosures. The extent of oxic/suboxic and anoxic zones, as indicated by the presence of nitrate as well as dissolved Mn and Fe_{tot}, within the profiles is indicated with blue and grey shading, respectively. Modelled concentration profiles are shown for both oxic/suboxic and anoxic conditions (solid lines). Note that for outside of the ring enclosure at S2 no removal rate constants were calculated as redox condition remained oxic throughout the profile and no denitrification occurred.

338 **Table 2** Average removal percentages calculated over the entire profile, median half-lives and associated interquartile ranges (IQR) for all TrOCs investigated in this study. Kruskal-
339 Wallis test statistics indicate whether removal rate constants obtained for oxic/suboxic conditions differed significantly from removal rate constants obtained under anoxic conditions. *N*
340 denotes the total number of profiles and *n* the number of profiles in which removal was insignificant. According to relative removal (%) and the redox dependency of removal rate
341 constants, TrOCs were grouped into four groups: (i) removal > 15%, significant redox influence on removal rate constants (ii) removal > 15% , insignificant redox influence on
342 removal rate constants (iii) removal ≤ 15%, insignificant redox influence on removal rate constants and group (iv) compounds that showed ambiguous behaviour. Note that individual
343 removal rate constants calculated from every (sub-) profile as well as median surface water concentrations of the investigated TrOCs are provided in the SM.

TrOC	Relative removal (%)	Kruskal-Wallis test statistics		Median $t_{1/2}$ ± IQR $t_{1/2}$ (d)		n/N	
		p - value	Chi square	oxic/suboxic	anoxic	oxic/suboxic	anoxic
Gabapentin[i] (GAB)	77±4	< 0.01	13.6	0.04±0.05	0.00±0.00	0/11	7/9
Bezafibrate[i] (BZF)	61±7	< 0.01	12.5	0.05±0.06	0.00±0.16	0/11	5/9
Acesulfame[i] (ACS)	66±7	< 0.01	8.0	0.05±0.02	-4.12±0.44	1/7	3/7
Benzotriazole[i] (BTA)	51±7	< 0.01	14.8	0.09±0.13	0.00±0.00	0/11	7/9
Diclofenac[i] (DCF)	36±9	< 0.01	9.7	0.16±0.13	0.00±0.00	3/11	8/9
Methylbenzotriazole[i] (MBT)	36±9	< 0.01	13.3	0.18±0.26	0.00±0.00	1/11	9/9
Primidon[i] (PRI)	32±10	< 0.01	7.9	0.43±0.14	0.00±0.00	4/11	9/9
4-Formylaminoantipyrin[iv] (FAA)	9±17	< 0.01	6.5	0.00±0.15	0.00±2.19	6/11	6/9
Metoprolol[iv] (MTP)	-6±17	0.04	4.1	0.23±0.14	0.00±0.43	3/11	4/9
				entire profile		entire profile	
Sulfamethoxazole[ii] (SMX)	46±9	0.08	3.1	0.29±0.18		1/12	
Diatrizoic acid[ii] (DTA)	33±10	0.10	2.7	0.32±0.22		3/12	
Venlafaxine[iii] (VLX)	14±12	0.17	1.9	0.00±0.74		5/8	
Carbamazepine[iii] (CBZ)	15±12	0.19	1.7	0.00±0.49		8/12	

344   Stability of TrOCs in the HZ varied widely with some TrOCs being readily attenuated in the HZ (i.e.

345   removal > 15% over the entire profile) and others being rather persistent (i.e. removal ≤ 15%). Similar to

346   the findings of previous field and laboratory studies (Burke et al., 2014; Wiese et al., 2011), removal rate

347   constants for the majority of TrOCs investigated showed a strong dependence on redox conditions. Based

348   on the redox dependency as well as relative removal within the HZ, TrOCs were grouped into (i)

349   compounds that were removed by more than 15% and showed redox-dependent removal rate constants (ii)

350   compounds that were removed by more than 15% and showed redox-independent removal rate constants,

351   (iii) compounds that were removed by less than 15% and (iv) compounds that showed ambiguous

352   behavior within the sampled profiles.

353   Compounds in group i comprised ACS, GAB, BZF, BTA, MBT, DCF and PRI. Data on the fate of the

354   anticonvulsant gabapentin in saturated sediments is limited but a laboratory column study showed that

355   oxic conditions promote GAB removal (Hellauer et al., 2017). Acesulfame, an artificial sweetener, was

356   originally suggested to act as an ideal wastewater tracer (e.g., Engelhardt et al., 2013). More recent

357   studies, however, demonstrated as well as the present study that the compound undergoes redox-

358   dependent attenuation, with higher removal observed under oxic conditions (Burke et al., 2014; Regnery

359   et al., 2015). Reported half-lives for ACS under oxic/suboxic redox conditions range from 0.21 d to 4.2 d,

360   exceeding the median half-life found in the HZ of River Erpe (0.05 d) by more than one order of

361   magnitude. The use of ACS as a tracer is therefore not recommended, especially if oxic to suboxic

362   conditions might occur along the flow path. Reported half-lives of bezafibrate, a lipid lowering agent,

363   range from 1.0 d in the transient storage zone of a natural river (Riml et al., 2013) to 1.9 d in a laboratory

364   flume study (Li et al., 2015) and are thus almost two orders of magnitude higher than the median half-life

365   calculated for oxic/suboxic conditions in the present study (0.05 d). The anti-corrosive agents

366   benzotriazole and its methyl analogue 5-methyl-1H-benzotriazole have both been shown to be relatively

367   stable in saturated sediments. (Liu et al., 2013), for instance, reported redox-dependent removal for MBT

368   and BTA in microcosms with half-lives of 60 d and 76 d for nitrate reducing conditions, while BTA was

369   found to be persistent in a column study that used hyporheic sediment (Burke et al., 2014). These findings

370   are in contrast to the data reported in the present study showing that both BTA and MBT undergo rapid

371   removal within the HZ. Among all investigated TrOCs, BTA and MBT were the only ones for which

372   concentrations strongly correlated with each other (adj. R^2 = 0.90, p-vlaue < 0.01), indicating that, in

373   principle, the same process seems to affect the removal of both compounds. A general redox dependency

374   of the removal of diclofenac, an analgesic, has been shown in both laboratory and field studies (Burke et

375   al., 2014; Wiese et al., 2011). Under oxic/suboxic conditions, reported half-lives ranged from 3 d to 36 d

376   within bank filtration settings (Henzler et al., 2014; Wiese et al., 2011). Shorter half-lives (0.13 d) were

377   observed in a column study (Burke et al., 2014), a value that agrees well with the half-life found in the

378   present study for oxic/suboxic conditions. Although the concentrations of primidone, an anticonvulsant,

379   did not decrease significantly in some of the oxic/suboxic sub-profiles (4 out of 11 profiles), overall mean

380   removal was found to be 32±10%. This was not expected as previous studies found half-lives for PRI in

381   the order of several years (Regnery et al., 2015).

382   Compounds of group ii comprised the anti-bacterial agent sulfamethoxazole as well as the X-ray contrast

383   agent diatrizoic acid. Both compounds were attenuated in the HZ, but calculated removal rate constants

384   did not depend on redox conditions. For SMX, this finding is in agreement with previous findings

385   indicating its removal under both oxic and anoxic conditions (Baumgarten et al., 2011). In a laboratory

386   flume study and during bank filtration, half-lives of 34 d and 22 d were reported for SMX respectively

387   (Henzler et al., 2014; Li et al., 2015) exceeding the median half-life found in this study (0.29 d) by

388   roughly two orders of magnitude. Removal of DTA during wastewater treatment was reported (Haiß and

389   Kümmerer, 2006) but limited data on removal rate constants in natural sediments is available.

390   The anticonvulsant carbamazepine and the neuro-active compound venlafaxine (group iii) were found to

391   be rather stable in the HZ of River Erpe. CBZ was previously reported to be very persistent in saturated

392   sediments (Bertelkamp et al., 2014; Henzler et al., 2014). Although removal of CBZ has been described

393   for iron-reducing conditions (Wiese et al., 2011), ambient exposure times to such redox conditions in the

394   present study were likely too short for the compound to be significantly removed. For VLX removal has

395   been demonstrated in the laboratory column study by Hellauer et al., (2017), but the compound was found

396   to be persistent in streams and during river bank filtration (Huntscha et al., 2013; Writer et al., 2013). It is

397   likely that residence times in the investigated section of the HZ were too short to achieve significant

398   attenuation for CBZ and VLX. Although median half-lives were zero for both compounds, in some

399   profiles concentrations of VLX and CBZ decreased significantly allowing the calculation of

400   comparatively low removal rate constants.

401   Similar inconsistent behaviour was also found for the compounds of group iv, the beta-blocker metoprolol

402   and 4-formylaminoantipyrin, a metabolite of the antipyretic drug dipyrone. Although MTP was persistent

403   in the transient storage zone of a natural river (Riml et al., 2013), half-lives of several hours were reported

404   in laboratory studies (Bertelkamp et al., 2014; Burke et al., 2014). Removal of 4-formylaminoantipyrin in

405   saturated sediments has been demonstrated in both laboratory and field studies with half-lives ranging

406   from 0.12 to 14 days (Burke et al., 2014; Wiese et al., 2011). Although overall removal for FAA and MTP

407   was insignificant, both showed positive removal during oxic/suboxic conditions and negative removal

408   rates (indicating concentrations increase) during anoxic conditions.

409   The order of relative stability of TrOCs encountered in the HZ of River Erpe partly differs from relative

410   stabilities described in other studies. For instance, CBZ was often found to be relatively more stable than

411   DCF (Burke et al., 2014; Wiese et al., 2011), which is in accordance with the findings of the present study.

412   In contrast, ACS has been found to be more stable than DCF (Burke et al., 2014; Regnery et al., 2015),

413   although in the present study DCF was more stable than ACS. Unsystematic findings with respect to

414   relative stabilities of TrOCs were mainly attributed to sediment heterogeneity and microbial community

415   diversity (Radke and Maier, 2014).

416   It should be further noted, that the calculation of removal rate constants in the present study is based on

417   field data collected under winter conditions with average hyporheic temperatures of 10°C (Figure SM-13).

418   Previous studies have shown that with increasing temperatures, removal rate constants increase (Burke et

419 al., 2014). However, with increasing temperatures redox zonation may also shift upwards thus limiting

420 exposure time to oxic/suboxic redox conditions and rendering the HZ less efficient in removing

421 compounds that show preferred removal under oxic/suboxic conditions.

422 In summary, in-situ removal rate constants of the majority of TrOCs in the HZ of River Erpe are one or

423 even two orders of magnitude higher compared to removal rates reported in previous studies. We found

424 that even compounds that were previously regarded as very stable, such as BTA and PRI, are retained in

425 the HZ. As sorption is generally not regarded to considerably influence removal of polar TrOCs (see SM

426 for detailed discussion and $logD_{ow}$ values), biotransformation is likely to be the dominant removal

427 mechanism for TrOCs in the HZ. Previous studies indicated that removal rate constants correlated

428 positively with microbial activity and TrOCs concentrations (Bertelkamp et al., 2016). The relatively high

429 removal rate constants in the HZ may thus be the results of site-specific characteristics of River Erpe, i.e.

430 high nutrient concentrations and high loads of TrOCs, high microbial activity in the upper centimetres of

431 the HZ as indicated by the steep redoxclines and the presence of a well-adapted microbial community.

4. Conclusion

The present study provides in-situ removal rate constants of several polar TrOCs in the HZ of an urban lowland stream. Compared to laboratory studies and bank filtration settings, removal rate constants of TrOCs in the HZ were relatively high and thus HZs may efficiently remove TrOCs along short flow paths. River restoration measures that explicitly aim at increasing hyporheic exchange in streams that are dominated by WWTP effluent may thus improve whole-stream TrOCs removal and hence water quality. We demonstrate that removal efficiency of the HZ is controlled by both residence times (i.e. advective transport velocity and the magnitude of groundwater-surface water exchange fluxes) and the reactivity of the respective TrOCs. For the majority of TrOCs, removal rate constants and thus removal efficiency of the HZ were significantly higher under oxic/suboxic conditions than under anoxic conditions. When predicting the fate of TrOCs in the HZ or assessing the relevance of the HZ with respect to whole-stream TrOCs attenuation, future studies should therefore consider exposure times to ambient redox conditions rather than overall residence time distributions in the HZ. For TrOCs that show redox-dependent biotransformation, relative removal may be increased if exposure times to oxic/suboxic conditions are enlarged.

The present study also suggests that high microbial activity promotes TrOCs removal. However, high microbial activity also leads to steep redox gradients and, for many TrOCs, is thus expected to limit the spatial extent of reactive zones in the HZ. More research is needed to understand the in-situ interactions between exchange fluxes, microbial metabolism and the extent of favourable "reactive" zones in the HZ. While we provide insights into the general fate of parent TrOCs in the HZ, future studies should also include transformation products and thus aim at closing mass balances along flow paths.

References

Baumgarten, B., Jährig, J., Reemtsma, T., Jekel, M., 2011. Long term laboratory column experiments to simulate bank filtration: Factors controlling removal of sulfamethoxazole. Water Res. 45, 211–220. https://doi.org/10.1016/j.watres.2010.08.034

Bertelkamp, C., Reungoat, J., Cornelissen, E.R., Singhal, N., Reynisson, J., Cabo, A.J., van der Hoek, J.P., Verliefde, A.R.D., 2014. Sorption and biodegradation of organic micropollutants during river bank filtration: A laboratory column study. Water Res. 52, 231–241. https://doi.org/10.1016/j.watres.2013.10.068

Bertelkamp, C., van der Hoek, J.P., Schoutteten, K., Hulpiau, L., Vanhaecke, L., Vanden Bussche, J., Cabo, A.J., Callewaert, C., Boon, N., Löwenberg, J., Singhal, N., Verliefde, A.R.D., 2016. The effect of feed water dissolved organic carbon concentration and composition on organic micropollutant removal and microbial diversity in soil columns simulating river bank filtration. Chemosphere 144, 932–939. https://doi.org/10.1016/j.chemosphere.2015.09.017

Boano, F., Harvey, J.W., Marion, A., Packman, A.I., Revelli, R., Ridolfi, L., Wörman, A., 2014. Hyporheic flow and transport processes: Mechanisms, models, and biogeochemical implications. Rev. Geophys. 52, 603–679. https://doi.org/10.1002/2012RG000417

Burke, V., Greskowiak, J., Asmuß, T., Bremermann, R., Taute, T., Massmann, G., 2014. Temperature dependent redox zonation and attenuation of wastewater-derived organic micropollutants in the hyporheic zone. Sci. Total Environ. 482, 53–61. https://doi.org/10.1016/j.scitotenv.2014.02.098

Engelhardt, I., Prommer, H., Moore, C., Schulz, M., Schüth, C., Ternes, T.A., 2013. Suitability of temperature, hydraulic heads, and acesulfame to quantify wastewater-related fluxes in the hyporheic and riparian zone. Water Resour. Res. 49, 426–440. https://doi.org/10.1029/2012WR012604

Fitzgerald, A., Roy, J.W., Smith, J.E., 2015. Calculating discharge of phosphorus and nitrogen with groundwater base flow to a small urban stream reach. J. Hydrol. 528, 138–151. https://doi.org/10.1016/j.jhydrol.2015.06.038

Gordon, R.P., Lautz, L.K., Briggs, M.A., McKenzie, J.M., 2012. Automated calculation of vertical pore-water flux from field temperature time series using the VFLUX method and computer program. J. Hydrol. 420, 142–158. https://doi.org/10.1016/j.jhydrol.2011.11.053

Greskowiak, J., Hamann, E., Burke, V., Massmann, G., 2017. The uncertainty of biodegradation rate constants of emerging organic compounds in soil and groundwater – A compilation of literature values for 82 substances. Water Res. 126, 122–133. https://doi.org/10.1016/j.watres.2017.09.017

Haiß, A., Kümmerer, K., 2006. Biodegradability of the X-ray contrast compound diatrizoic acid, identification of aerobic degradation products and effects against sewage sludge micro-organisms. Chemosphere 62, 294–302. https://doi.org/10.1016/j.chemosphere.2005.05.007

Harvey, J.W., Böhlke, J.K., Voytek, M.A., Scott, D., Tobias, C.R., 2013. Hyporheic zone denitrification: Controls on effective reaction depth and contribution to whole-stream mass balance: Scaling hyporheic flow controls on stream denitrification. Water Resour. Res. 49, 6298–6316. https://doi.org/10.1002/wrcr.20492

Hellauer, K., Mergel, D., Ruhl, A., Filter, J., Hübner, U., Jekel, M., Drewes, J., 2017. Advancing sequential managed aquifer recharge technology (SMART) using different intermediate oxidation processes. Water 9, 221. https://doi.org/10.3390/w9030221

Henzler, A.F., Greskowiak, J., Massmann, G., 2014. Modeling the fate of organic micropollutants during river bank filtration (Berlin, Germany). J. Contam. Hydrol. 156, 78–92. https://doi.org/10.1016/j.jconhyd.2013.10.005

Hesslein, R.H., 1976. An in situ sampler for close interval pore water studies. Limnol. Oceanogr. 21, 912–914.

500   Hoppe-Jones, C., Dickenson, E.R.V., Drewes, J.E., 2012. The role of microbial adaptation and
501   biodegradable dissolved organic carbon on the attenuation of trace organic chemicals during
502   groundwater recharge. Sci. Total Environ. 437, 137–144.
503   https://doi.org/10.1016/j.scitotenv.2012.08.009
504   Huntscha, S., Rodriguez Velosa, D.M., Schroth, M.H., Hollender, J., 2013. Degradation of polar organic
505   micropollutants during riverbank filtration: Complementary results from spatiotemporal sampling
506   and push–pull tests. Environ. Sci. Technol. 47, 11512–11521. https://doi.org/10.1021/es401802z
507   Krause, S., Lewandowski, J., Grimm, N.B., Hannah, D.M., Pinay, G., McDonald, K., Martí, E., Argerich,
508   A., Pfister, L., Klaus, J., Battin, T., Larned, S.T., Schelker, J., Fleckenstein, J., Schmidt, C.,
509   Rivett, M.O., Watts, G., Sabater, F., Sorolla, A., Turk, V., 2017. Ecohydrological interfaces as hot
510   spots of ecosystem processes. Water Resour. Res. 53, 6359–6376.
511   https://doi.org/10.1002/2016WR019516
512   Lewandowski, J., Putschew, A., Schwesig, D., Neumann, C., Radke, M., 2011. Fate of organic
513   micropollutants in the hyporheic zone of a eutrophic lowland stream: Results of a preliminary
514   field study. Sci. Total Environ. 409, 1824–1835. https://doi.org/10.1016/j.scitotenv.2011.01.028
515   Li, Z., Sobek, A., Radke, M., 2015. Flume experiments to investigate the environmental fate of
516   pharmaceuticals and their transformation products in streams. Environ. Sci. Technol. 49, 6009–
517   6017. https://doi.org/10.1021/acs.est.5b00273
518   Liu, Y.-S., Ying, G.-G., Shareef, A., Kookana, R.S., 2013. Biodegradation of three selected benzotriazoles
519   in aquifer materials under aerobic and anaerobic conditions. J. Contam. Hydrol. 151, 131–139.
520   https://doi.org/10.1016/j.jconhyd.2013.05.006
521   McCallum, A.M., Andersen, M.S., Rau, G.C., Acworth, R.I., 2012. A 1-D analytical method for
522   estimating surface water-groundwater interactions and effective thermal diffusivity using
523   temperature time series. Water Resour. Res. 48. https://doi.org/10.1029/2012WR012007
524   Munz, M., Oswald, S.E., Schmidt, C., 2011. Sand box experiments to evaluate the influence of subsurface
525   temperature probe design on temperature based water flux calculation. Hydrol. Earth Syst. Sci. 15,
526   3495–3510. https://doi.org/10.5194/hess-15-3495-2011
527   Pal, A., He, Y., Jekel, M., Reinhard, M., Gin, K.Y.-H., 2014. Emerging contaminants of public health
528   significance as water quality indicator compounds in the urban water cycle. Environ. Int. 71, 46–
529   62. https://doi.org/10.1016/j.envint.2014.05.025
530   R Core Team, 2016. R: A language and environment for statistical computing. R Foundation for Statistical
531   Computing, Vienna, Austria. URL https://www.R-project.org/.
532   Radke, M., Maier, M.P., 2014. Lessons learned from water/sediment-testing of pharmaceuticals. Water
533   Res. 55, 63–73. https://doi.org/10.1016/j.watres.2014.02.012
534   Regnery, J., Wing, A.D., Alidina, M., Drewes, J.E., 2015. Biotransformation of trace organic chemicals
535   during groundwater recharge: How useful are first-order rate constants? J. Contam. Hydrol. 179,
536   65–75. https://doi.org/10.1016/j.jconhyd.2015.05.008
537   Riml, J., Wörman, A., Kunkel, U., Radke, M., 2013. Evaluating the fate of six common pharmaceuticals
538   using a reactive transport model: Insights from a stream tracer test. Sci. Total Environ. 458–460,
539   344–354. https://doi.org/10.1016/j.scitotenv.2013.03.077
540   Schwarzenbach, R.P., Escher, B.I., Fenner, K., Hofstetter, T.B., Johnson, A.C., von Gunten, U., Wehrli,
541   B., 2006. The Challenge of Micropollutants in Aquatic Systems. Science 313, 1072–1077.
542   https://doi.org/10.1126/science.1127291
543   Wiese, B., Massmann, G., Jekel, M., Heberer, T., Dünnbier, U., Orlikowski, D., Grützmacher, G., 2011.
544   Removal kinetics of organic compounds and sum parameters under field conditions for managed
545   aquifer recharge. Water Res. 45, 4939–4950. https://doi.org/10.1016/j.watres.2011.06.040
546   Writer, J.H., Antweiler, R.C., Ferrer, I., Ryan, J.N., Thurman, E.M., 2013. In-Stream Attenuation of
547   Neuro-Active Pharmaceuticals and Their Metabolites. Environ. Sci. Technol. 47, 9781–9790.
548   https://doi.org/10.1021/es402158t
549   Young, P.C., Pedregal, D.J., Tych, W., 1999. Dynamic harmonic regression. J. Forecast. 18, 369–394.

550   Zietzschmann, F., Aschermann, G., Jekel, M., 2016. Comparing and modeling organic micro-pollutant
551   adsorption onto powdered activated carbon in different drinking waters and WWTP effluents.
552   Water Res. 102, 190–201. https://doi.org/10.1016/j.watres.2016.06.041
553   Zietzschmann, F., Mitchell, R.-L., Jekel, M., 2015. Impacts of ozonation on the competition between
554   organic micro-pollutants and effluent organic matter in powdered activated carbon adsorption.
555   Water Res. 84, 153–160. https://doi.org/10.1016/j.watres.2015.07.031
556

565